Available online at www.sciencedirect.com
SCIENCE DIRECT®
ELSEVIER
Journal of Nuclear Materials 337–339 (2005) 221–226
journal of nuclear materials
www.elsevier.com/locate/jnucmat

3D edge energy transport in stellarator configurations

N. McTaggart [a], R. Zagórski [b,*], X. Bonnin [a], A. Runov [a], R. Schneider [a], T. Kaiser [c], T. Rognlien [c], M. Umansky [c]

[a] Max-Planck-Institut für Plasmaphysik, Teilinstitut Greifswald, EURATOM Association, Wendelsteinstraße 1, D-17491 Greifswald, Germany
[b] Institute of Plasma Physics and Laser Microfusion, P.O. Box 49, Warsaw, Poland
[c] Lawrence Livermore National Laboratory, Livermore, CA 94551, USA

Abstract

The finite difference discretization method is used to solve the electron energy transport equation in complex 3D edge geometries using an unstructured grid. This grid is generated by field-line tracing to separate the radial and parallel fluxes and minimize the numerical diffusion connected with the strong anisotropy of the system. The influence of ergodicity on the edge plasma transport in the W7-X stellarator is investigated in this paper. Results show that the combined effect of ergodicity and the radial plasma diffusion leads to the efficient smoothing of the temperature profiles in the finite-β case.
© 2004 Elsevier B.V. All rights reserved.

PACS: 02.60.Lj; 02.70.B; 52.55.H; 52.65
Keywords: Edge plasma; Island divertor; Power deposition; Stochastic boundary

1. Introduction

Modeling in ergodic regions in magnetized plasmas has special difficulties due to the strong anisotropy of the transport and the complex geometry of the computational domain. In the present work a method is developed to model electron heat conduction in the plasma edge of fusion experiments.

We employ the finite difference discretization method which allows the numerical simulation of electron energy transport in complex 3D edge geometries using a custom-tailored unstructured grid [1]. This grid is generated by field-line tracing to guarantee complete isolation between the large parallel transport along magnetic field B and that perpendicular to B. Therefore the radial and parallel fluxes are almost perfectly separated which minimizes the numerical diffusion connected with the strong anisotropy of the system ($\Gamma_{\parallel}/\Gamma_{\perp} \sim 10^7$).

The problem of ergodicity is handled by using local magnetic coordinates [2]. This allows a discretization of the transport equation as long as the toroidal distance between the mesh points is well below the Kolmogorov length. The use of local magnetic coordinates allows a complete description of the system without additional approximation, however, a full metric tensor with non-diagonal terms [2] has to be considered.

A finite difference code (FINDIF) has been developed for modelling 3D plasma edge physics including ergodic effects [1,3]. Grids were generated in a vacuum

* Corresponding author. Tel.: +48 22 6381460; fax: +48 22 6668372.
E-mail address: zagorski@ifpilm.waw.pl (R. Zagórski).

0022-3115/$ - see front matter © 2004 Elsevier B.V. All rights reserved.
doi:10.1016/j.jnucmat.2004.10.030

field (low ergodicity) and a finite-β field (high ergodicity) for a W7-X configuration. The code has been applied to the W7-X case, though it is applicable to many fusion experiments (TEXTOR-DED, NCSX).

2. Transport model and numerical method

In the present paper we restrict ourselves only to the heat balance equation for electrons. In general curvilinear coordinates x^i the electron energy equation can be written in the form of a conservation of a fluid property $f(\equiv 3nT_e/2)$

$$\frac{\partial f}{\partial t} = \frac{1}{\sqrt{g}}\frac{\partial}{\partial x^i}\sqrt{g}\left(D^{ij}\frac{\partial f}{\partial x^j} - V^i f\right) - \nu f + S^{(f)}. \quad (1)$$

Here, g is the metric determinant and D^{ij} is the diffusion tensor appropriate for f ($D_\perp \equiv \kappa_\perp$, $D_\parallel \equiv \kappa_\parallel$, with $\kappa_\perp$ and $\kappa_\parallel$ being the anomalous perpendicular and classical parallel thermal conductivity coefficients respectively), ν is the electron heat loss rate and $S^{(f)}$ is a generalized heat source. In the following we assume that the flow velocity, V^i, is zero (more general cases have been already treated in [1]).

For a coordinate system with one coordinate (e.g. x^3) along the magnetic field line the parallel flux has only one non-vanishing component and the resulting form of the diffusion tensor is [2]:

$$D^{ij} = D_\perp g^{ij} + (D_\parallel - D_\perp)(h^3)^2\delta_3^i\delta_3^j,$$

(δ_j^i is a Kronecker symbol). Generally we are forced to use local magnetic coordinates because the applicability of a single coordinate system is limited by some toroidal distance (Kolmogorov length).

In order to handle ergodicity and the strong anisotropy of the system we use a finite difference method in which we solve the discretized transport equation at points generated along the field lines. The computational process has 4 main stages and has been described in detail in Refs. [1,3].

Mesh generation: Starting from a magnetic field configuration data file we use a field line tracing code to trace field lines around the torus and generate points at regular toroidal intervals.

Triangulation: Using a modified Delaunay algorithm we triangulate the mesh to determine the connectivities between the points (the neighborhood array for each point).

Metric coefficients: Using a modified field line tracing code [3] we generate the metric coefficients for each mesh point.

Transport code: The transport code contains the discretized form of the transport equation. It solves the transport equation as a system of simultaneous equations, by iteration, in order to obtain a steady state solution.

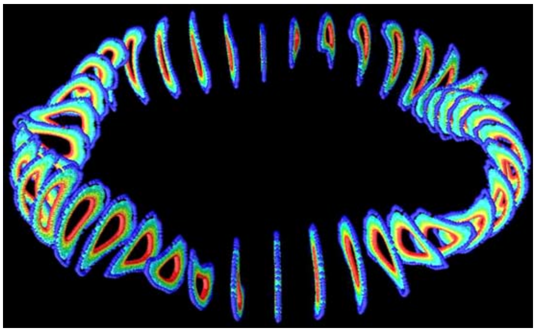

Fig. 1. 3D Electron temperature solution in a W7-X configuration.

A 3D temperature solution for the W7-X stellarator obtained with the FINDIF code is shown in Fig. 1. It should be noted that generating large meshes is time consuming but is done only once for a given magnetic configuration.

3. Results

In the present paper we investigate the effects of ergodicity on energy transport in the edge region of the W7-X experiment. Studies were done on meshes generated in a vacuum field, where there is small ergodicity, and in a finite-β field (β = 4%) with relatively large ergodicity (typical Kolmogorov length $\sim 10 \rightarrow 30$ m). We point out that the magnetic field was calculated with the VMEC code. In Fig. 2 we show 2D temperature profiles on Poincaré plots at $\phi = 0°$ from the vacuum (left) and finite-β (right) meshes. Each mesh point is colored according to the steady state temperature. In both cases we prescribe a constant temperature 200 eV at the inner boundary of the integration domain, 10 eV at the outer boundary, and sheath conditions at the divertor plates [4]. Radial diffusivity was $1\,\mathrm{m^2\,s^{-1}}$ and the particle density was $10^{20}\,\mathrm{m^{-3}}$.

In the vacuum case we can recognize the island structure in the solution with relatively high plasma temperatures at the target plates ($\sim$50 eV). However, looking at the finite-β solution, we can see the strong broadening of the temperature profiles and smearing out of the islands (relatively broad cold region in blue in front of the target plates). In order to understand these 2D plots, and the reason for differences between the vacuum and finite-β cases we can analyze the full 3D solutions shown in Figs. 3 and 4.

We present the solutions in the form of temperature distributions along field lines. In both cases the field lines have been normalized with respect to their own length. Every line in the plot shows temperature along one (normalized) field line. In the same figures we have included

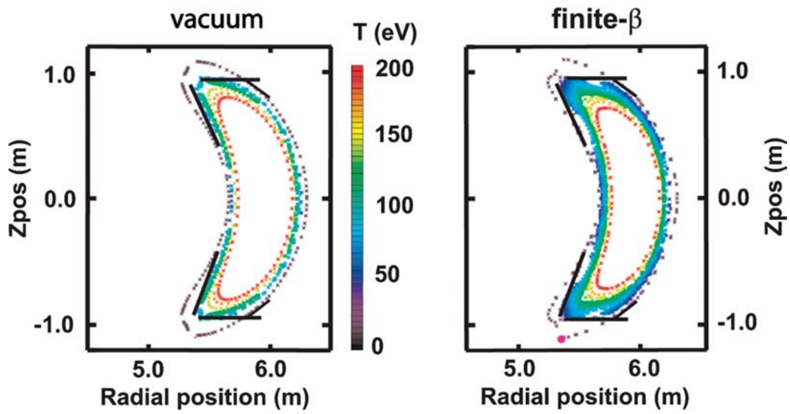

Fig. 2. Temperature solution on a Poincaré plot for the vacuum and the finite-β case.

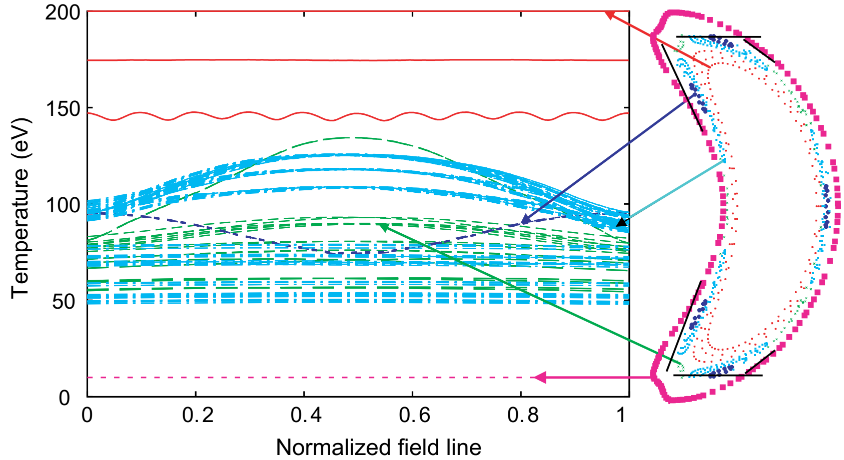

Fig. 3. Solution on the vacuum mesh. This mesh has no closed ergodic field lines and there is a closed flux surface in the center of each island (dark blue (overlapping) curves).

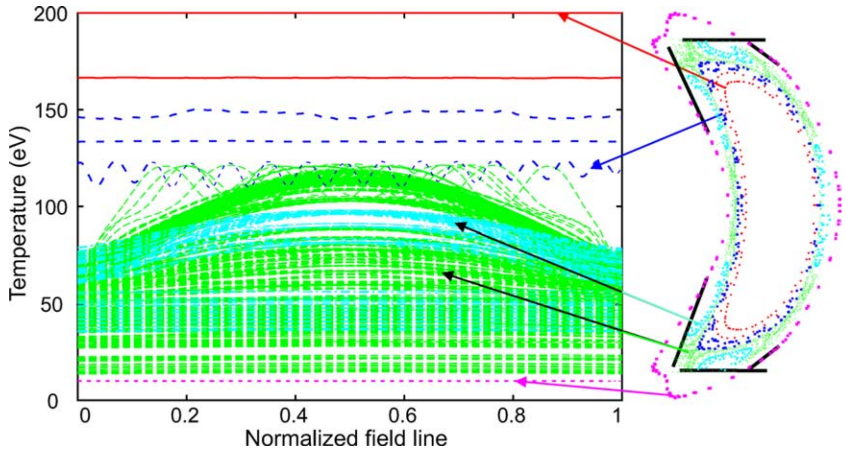

Fig. 4. Solution on the finite-β mesh. This mesh has three closed ergodic field lines surrounding the plasma core (dark blue curves), and no closed flux surfaces in the islands.

Poincaré plots ($\phi = 0°$) of mesh points. The different colors (and arrows) show the correspondence between the normalized field lines in the temperature solutions and the position of the field lines in space. Different colors are only labels which distinguish different groups of field lines with different starting points, different topology (close, open, ergodic, ...) and/or different position in space.

Vacuum Case: Looking at the 3D temperature solution for vacuum mesh (Fig. 3) we can see a gap in the temperature profiles between the closed field lines in the core region (red field lines) and the open field lines in the edge layer (blue and green field lines). This gap inhibits transport from the core to the edge.

The left figure in Fig. 2 shows a 2D temperature solution on a Poincaré plot from the vacuum mesh. Comparing Fig. 3 with the vacuum case in Fig. 2 we can see that the red curves in Fig. 3 are the three core flux surfaces of which the outermost flux surface is the wavy line at $\sim$150 eV.

The light blue curves are the open flux surfaces in the islands. Within each island the solution shows an ordered temperature gradient across the flux surfaces. The open flux surfaces in the islands contain many field lines of different lengths. The triple grouping of light blue contours which peak in the range $100 \rightarrow 125$ eV correspond to field lines on successive flux surfaces, e.g. the highest group (peaking at $\sim$125 eV) lie on the outermost flux surfaces of the islands. The flatter light blue contours in the range $50 \rightarrow 80$ eV are much shorter open field lines in the islands. Inspection of the corresponding Poincaré plot shows that the field lines forming the outermost flux surfaces of the islands come quite close to the last closed flux surface in the core and in Fig. 3 the temperature peaks of these field lines reach up to $\sim$125 eV. But on the plane of the Poincaré plot the ends of these flux surfaces are also in direct contact with the wall. Consequently, in the solution the lowest points on these open field lines reach down to $\sim$50 eV.

The dark blue curves are the five field lines which each form one closed flux surface in each island. The Poincaré plot shows that the closed flux surface inside each island is exposed to the outer boundary which is held constant at 10 eV, and this is the cause of the dip.

The green curves are the open field lines elsewhere in the edge region. Note the presence of long open field lines in green (2 lines in our mesh) which come close to the plasma core and peak at $\sim$135 eV.

Finite-β Case: Next we deal with a finite-β case in which there are strong ergodic effects around the separatrix of the main island chain. Fig. 4 shows a 3D temperature solution along the normalized field lines together with the Poincaré plot ($\phi = 0°$) of mesh points. The blue points (in the Poincaré plot), which lie on the closed ergodic field lines, represent the thin ergodic layer which surrounds the plasma core. The green points reveal the position of the separatrix and, especially at the top and bottom, show an x-point like formation. Points which are near to these x-formations lie on long open field lines (green) which show oscillatory behavior.

Fig. 4 shows that in the finite-β case there is a significant overlap (mixing) of the field lines in temperature space. In real space this new heat flux pattern drives additional radial transport with the result that regions which were previously inaccessible are now filled by flux tubes.

In the top half of the plot the closed field lines in the core region can be seen. These red curves are the two core flux surfaces. Next, we have three dark blue curves forming the ergodic layer. The outermost closed ergodic field line surrounding the core is a blue wavy line at $\sim$120 eV. We point out that only those field lines which are much longer than the Kolmogorov length ($\sim 10 \rightarrow 30$ m) can 'see' the ergodicity in the system and these field lines exhibit oscillations. The closed field line at $\sim$135 eV is almost flat because it is relatively short.

Below these closed field lines there is the dense group of open field lines in the edge region (green), and the islands (light blue). Most of these form roughly parabolic curves but a few form oscillating curves because they are long enough to see the ergodicity in the system. Note that many of the temperature contours on these open field lines overlap the outermost closed ergodic field line. The general trend of open field lines is that for longer field lines the temperature profiles are more parabolic, and if a field line is long enough to 'see' the ergodicity then it is 'ergodic' and exhibits oscillations.

Inspection of Fig. 4 indicates that in the finite-β case there is strong mixing of the field lines in temperature space as a result of the enhancement in radial transport. It can be also seen in the 2D temperature distribution at the Poincaré plot at $\phi = 0°$ (Fig. 2 (right)). There is a broadening of the temperature profiles in the edge and the island structures are smeared out (compared to the vacuum case).

It is difficult to precisely compare the vacuum and finite-β meshes because they have different structures but the most notable differences are the isolated groups of lines in the vacuum solution and the gap, at $\sim$140 eV, between the closed core field lines and the open edge field lines. This represents a small radial transport in the vacuum case. In the finite-β case there is considerable overlapping of the temperature contours of the open field lines with the outermost closed ergodic field line. This represents a feeding of the open field lines by contact with the ergodic layer in temperature space which then also drives radial fluxes in real space. In addition, the temperatures at the ends of the open field lines are lowered in the finite-β case because, due to enhanced radial transport, the heat is deposited over a larger wall/target area.

Transport effects: In order to gain more insight into the mechanism of the energy transport in the plasma edge in the presence of ergodicity (finite-β), we made some parametric studies. First, we varied the boundary condition in the core, that is, the temperature at the points on the innermost flux surface ($T_{\text{core}} = 100$ and 300 eV, in comparison to the standard 200 eV case). Changing the core boundary condition represents a variation in the parallel transport ($\chi_{\|}$) but not in the radial transport ($\chi_{\perp}$). The result is a scaling of the temperature solutions but the relative positions of the structures in the core and edge regions remain unchanged, meaning that the solutions are to a large extent self-similar.

Next we varied the radial transport ($\chi_{\perp} = 0.1$ and $0.01\,\text{m}^2/\text{sec}$). This time the core boundary temperature was held constant at such a level that the input energy flux was almost the same as in the case $\chi_{\perp} = 1\,\text{m}^2/\text{sec}$ ($Q_{\text{inp}} \approx 8.2\,\text{MW}$). The results show that as the radial transport is reduced there is a progressive decoupling of the transport from the ergodic zone surrounding the core to the edge. Also, the temperature profiles along the field lines get flatter since the parallel transport becomes more important. Consequently, the intersection of long and hot field lines creates a hot spot pattern at the target plates (Fig. 5). This scan underlines the fact that the broadening effect of temperature profiles is driven also by radial transport and not only by geometrical interweaving which would be unaffected by varying the transport. Therefore, the smoothing of the temperature solution in the islands in the finite-β case is due to an indirect ergodic effect. The ergodicity triggers the cascading of energy into regions which were inaccessible in the vacuum case. However, ergodicity does not directly enhance transport on short field lines because the vast majority of these field lines are much shorter than the Kolmogorov length.

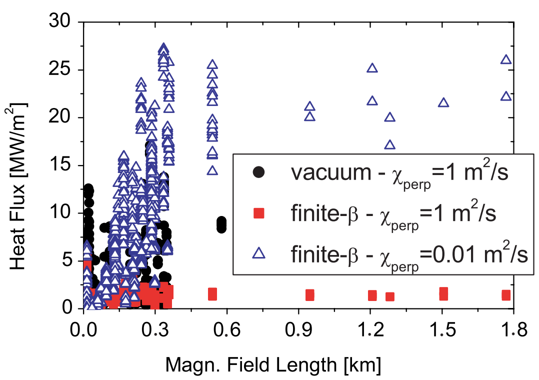

Fig. 5. Power load on the divertor target plates in W7-X. The black points: vacuum case. The red points: finite-β case ($\chi_{\perp} = 1\,\text{m}^2\,\text{s}^{-1}$). The blue points: finite-β case ($\chi_{\perp} = 0.01\,\text{m}^2\,\text{s}^{-1}$).

Fig. 5 shows heat fluxes at the target plates in the W7-X stellarator. The points in Fig. 5 lie grouped in columns because the open field lines are traced from similar sets of start points on similar cuts in the device, and the multiple symmetry of W7-X causes field line lengths to fall into groups.

The average flux on an open field line end point is $\sim 2.6\,\text{MW/m}^2$ for the typical radial transport ($\chi_{\perp} = 1\,\text{m}^2\,\text{s}^{-1}$), well below the engineering limits. However in the case of the reduced transport ($\chi_{\perp} = 0.01\,\text{m}^2\,\text{s}^{-1}$), when the influence of ergodicity is negligible, the fluxes are unacceptably larger, revealing the hot spot structure of the heat deposition.

4. Conclusions

In this paper the finite difference method implemented in the numerical code FINDIF is used to solve energy transport in the 3D boundary layer of fusion devices. The method is based on the concept of local magnetic coordinates and in order to separate the radial and parallel transport grid points are generated along magnetic field lines. Studies were done to investigate the W7-X configuration with the presence of ergodicity, which is caused by finite-β effects which result from the plasma pressure. Results show that the W7-X finite-β case allowed cascading of energy into regions which were inaccessible in the vacuum case. Radial transport causes further broadening of the temperature profiles. At the target plates this produces, as a surface effect, a spreading of the power load and a reduction of the peak power. The island structures are not prominent in the solution, being masked by the general flattening of the temperature profile in the edge region. It should be noted that this is not a direct effect of ergodicity, but an indirect effect where the dominant transport to the divertor plates is done through field lines which are much shorter than the Kolmogorov length. These field lines cannot exhibit ergodic effects.

By investigation of the energy fluxes to the divertor plates it was found that the fluxes in the finite-β case are much lower that the engineering constraints for the typical values of the radial transport ($\chi_{\perp} \sim 1\,\text{m}^2\,\text{s}^{-1}$). The fluxes are spread more or less uniformly over magnetic field lines of different lengths. It should be noted, however, that the parallel fluxes are determined by the field line length, longer field lines play a greater role in removing heat from the plasma core because they have more contact with the ergodic region surrounding the plasma core. We stress also that in the case of reduced radial transport the peak power load would be very high.

References

[1] R. Zagorski et al., Finite Difference Scheme for Solving General 3D Convection–Diffusion Equation, presented at the 18th ICNSP Conference, Cape Cod, September 2003, USA, submitted for publication, CPC.

[2] A.M. Runov et al., Phys. Plasmas 8 (3) (2001) 916.

[3] N. McTaggart, Finite Difference Code for 3D Edge Plasma Modelling, PhD thesis (2003) (http://www.ipp.mpg.de/~taggart/thesis.html).

[4] P.C. Stangeby, G.M. McCracken, Nucl. Fusion 30 (1990) 1225.